Bulletin of Electrical Engineering and Informatics
Vol. 14, No. 4, August 2025, pp. 3175~3188
ISSN: 2302-9285, DOI: 10.11591/eei.v14i4.9300

Development of classification model for thoracic diseases with chest X-ray images using deep convolutional neural network

Kennedy Okokpujie[1,2], Tamunowunari-Tasker Anointing[1], Adaora Princess Ijeh[3], Imhade Princess Okokpujie[4,5], Mary Oluwafeyisayo Ogundele[6], Oluwadamilola Oguntuyo[7]
[1]Department of Electrical and Information Engineering, College of Engineering, Covenant University, Ota, Nigeria
[2]Africa Centre of Excellence for Innovative and Transformative STEM Education, Lagos State University, Lagos, Nigeria
[3]Department of Computer and Information Science, College of Science and Technology, Covenant University, Ota, Nigeria
[4]Department of Mechanical and Mechatronics Engineering, Afe Babalola University, Ado Ekiti, Nigeria
[5]Department of Mechanical and Industrial Engineering Technology, University of Johannesburg, Johannesburg, South Africa
[6]Department of Critical Network and Security Solutions, Unified Payment, Idowu Martins, Victoria Island, Lagos, Nigeria
[7]Department of Mathematics, College of the Holy Cross, Worcester, United States

Article Info

Article history:

Received Sep 15, 2024
Revised Jun 6, 2025
Accepted Jul 5, 2025

Keywords:

Chest X-ray
Classification
Convolutional neural networks
Diagnosis
Lung disease

ABSTRACT

Thoracic disease is a medical condition in the chest wall region. Accurate thoracic disease diagnosis in patients is critical for effective treatment. Atelectasis, mass, pneumonia, and pneumothorax are thoracic diseases that can lead to life-threatening conditions if not detected and treated early enough. When diagnosing these diseases, human expertise can also be susceptible to errors due to fatigue or emotional factors. This research proposes developing a real-time deep learning-based classification model for thoracic diseases. Three deep convolutional neural network (CNN) models - MobileNetV3Large, ResNet-50, and EfficientNetB7 - were evaluated for classifying thoracic diseases from chest X-ray images. The models were tested in 5-class (atelectasis, mass, pneumothorax, pneumonia, and normal), 4-class (atelectasis, pneumothorax, pneumonia, and normal), and 3-class (atelectasis, pneumonia, and normal) modes to assess the impact of high interclass similarity. Retrained MobileNetV3Large achieved the highest classification accuracy: 75.72% next to ResNet-50 (75.2%) and last EfficientNetB7 (73.03%). For the 4-class, EfficientNetB7 (88.08%) led with MobileNetV3Large in the last (87.08%), but MobileNetV3Large led the 3-way with 97.88% with EfficientNetB7 again in the last (96.55%). These results indicate that MobileNetV3 can effectively distinguish and diagnose thoracic diseases from chest X-rays, even with interclass similarity and supports the use of computer-aided detection systems in thoracic disease classification.

Corresponding Author:

Kennedy Okokpujie
Department of Electrical and Information Engineering, College of Engineering, Covenant University
Km. 10 Idiroko Road, Canaan Land, Ota, Ogun State, Nigeria
Email: kennedy.okokpujie@covenantuniversity.edu.ng

1. INTRODUCTION

Thoracic disorders encompass a wide range of potentially life-threatening conditions affecting the heart, lungs, esophagus, mediastinum, chest wall, and great vessels. According to the World Health Organization (WHO), pneumonia is particularly critical among these. Pneumonia, a viral or bacterial infection, is a leading cause of death in children globally, especially in low and middle-income countries [1]. These statistics highlight the urgent need for accurate and accessible diagnostic tools. CXRs are the preferred

diagnostic tool for thoracic diseases such as pneumonia and tuberculosis and signs of heart failure like cardiomegaly (enlarged heart), pulmonary edema (fluid in the lungs) and lung cancer indications such as mass and nodules. This is because CXR's are readily accessible in most healthcare facilities, even in remote or resource-constrained settings. Compared to more advanced imaging techniques like CT scans or MRIs, CXRs offer a cost-effective and low-radiation alternative. However, traditional CXR interpretation relies on the skill and experience of radiologists, who can be susceptible to limitations. Radiologists are not infallible and can make mistakes in diagnosing chest X-rays, especially when dealing with high workload, fatigue, or complex cases requiring more attention and analysis [2].

The demand for radiologists often exceeds the supply, especially in remote or rural areas with a shortage of qualified and experienced radiologists. This can create disparities in access to accurate and timely diagnosis, as patients may have to wait longer or travel farther to get their chest X-rays read and interpreted [3]. The time it takes to get a chest X-ray result can significantly impact the patient's outcome, as some diseases may require prompt and urgent treatment to prevent complications or death. However, due to the limited number and availability of radiologists, there may be delays in getting the chest X-rays read and interpreted, affecting the quality of care and patient satisfaction [4].

Accurate classification of thoracic diseases from chest X-ray images is critical for timely and effective treatment. Traditional CXR interpretation methods rely heavily on the expertise of radiologists, who can be susceptible to human error, particularly under high workloads and fatigue. The availability of radiologists is limited, especially in rural and remote areas, leading to delays in diagnosis and treatment. Conventional diagnostic processes can be time-consuming and resource-intensive, impacting patient care and satisfaction [5]-[7]. Therefore, deep learning approaches like convolutional neural networks (CNNs), which offer promising solutions to these challenges by improving accuracy, efficiency, and accessibility in CXR analysis, are needed.

According to Xue *et al.* [8], the prevalence of atelectasis in hospitalized patients can be as high as 90% postoperatively. Radiologists often find it challenging to differentiate atelectasis from other conditions like pleural effusion or pneumonia due to similar radiographic appearances. AI models, particularly deep learning, can provide more consistent and precise analysis, thereby reducing diagnostic errors. Pneumothorax is a medical condition characterized by air in the pleural space, causing the lung to collapse partially or completely. Advances in AI, particularly deep learning algorithms, aim to enhance the accuracy of pneumothorax detection by identifying subtle changes and patterns in chest X-ray images that human radiologists may miss [9]. Early and accurate diagnosis of lung mass is crucial, especially for malignant masses, to improve patient outcomes through timely and appropriate interventions. Research indicates that incorporating AI into diagnostic workflows can enhance the ability to identify and classify lung masses accurately [9].

Pneumonia is an inflammatory condition of the lung affecting the alveoli, typically caused by bacterial, viral, or fungal infections. It can involve any part of the lungs, though bilateral lower lobe involvement is common. The challenge for radiologists in diagnosing pneumonia is that it can present with radiographic features similar to other conditions, such as atelectasis or pulmonary edema. AI systems can improve diagnostic accuracy by identifying specific patterns and anomalies in CXR images that may be subtle or difficult for human observers to detect. Studies have demonstrated the efficacy of AI models in enhancing the detection and classification of pneumonia, facilitating better clinical decision-making and patient care [5].

CXR is the most common and widely used imaging modality for diagnosing and screening various thoracic diseases, such as pneumonia, tuberculosis, lung cancer, and pleural effusion [3]. CXRs are relatively inexpensive, easy to acquire, and non-invasive compared to other imaging techniques like CT and MRI. However, interpreting CXR images is challenging and requires expert knowledge and experience. The demand for CXR interpretation is increasing due to the growing prevalence of respiratory diseases and the limited availability of radiologists. By leveraging artificial neural networks, deep learning models can automatically analyze chest X-ray images, extract intricate features, and highly accurately classify thoracic diseases [6], [10].

CNNs are a deep learning model capable of processing pictures and extracting valuable data. They consist of multiple layers of artificial neurons that apply mathematical operations to the input data, such as convolution, pooling, and activation [3]. These operations help reduce the data's dimensionality and enhance the most relevant features. Using [9] as a case study, which used the ResNet-50 architecture to classify over 100,000 frontal-view images with eight common thoracic disease labels as a benchmark, CNN architectures have shown remarkable accuracy in classifying common diseases that affect the lungs and the heart, such as pneumonia and cardiomegaly. These diseases have distinctive visual features that CNNs can detect, such as opacities, enlargement, and cavities.

In transfer learning, the initial layers of the pre-trained models are often frozen, making their weights static during the training process. In contrast, the later layers might not be frozen depending on the complexity of the task to allow for adjustment to higher-level features [10].

Custom layers may be added to the model to address the specific requirements of the new task. For instance, a new fully connected layer can be added at the network's end to classify the specific categories in the new dataset.

In the case of thoracic diseases, [11] explored transfer learning using pre-trained AlexNet, MobileNetV2 and ResNet-50 and 101 models for classifying diverse lung-related diseases. They compare the performance of fine-tuning and freezing pre-trained layers, offering insights into optimizing transfer learning strategies for different tasks with remarkable results.

The design of MobileNetV3 incorporates advancements from both MobileNetV2 and a new architecture search technique called NetAdapt, ensuring an optimal balance between computational efficiency and accuracy. Its streamlined architecture is particularly beneficial when handling large medical image datasets, where computational resources and inference speeds are critical. MobileNetV3Large integrates Squeeze-and-Excitation (SE) modules to amplify the representational capacity of its network. SE modules adaptively adjust the model's channel-specific feature responses. This is accomplished by explicitly modelling the interdependencies between channels. This is accomplished via a squeeze operation to compress the spatial dimensions into a channel descriptor and an excitation operation to scale the channel-specific properties. This approach allows the network to focus on the most relevant elements, enhancing its ability to detect meaningful input patterns [12]. The model in [13] diagnoses COVID-19 from chest X-ray (CXR) images. The researchers developed the COV-MobNets model, MobileNetV3Large, which was utilised as part of an ensemble of mobile networks.

ResNet50, short for residual network with 50 layers, and introduced by [14] is one of the most renowned deep learning models due to its exceptional performance in image classification tasks. In the network, each residual block typically consists of three layers: a 1×1 convolution, a 3×3 convolution, and another 1×1 convolution. The output of these layers is then added to the input of the block, forming a shortcut connection that allows gradients to flow directly through the network. The researchers in [15] used ResNet50 to identify pneumonia, tuberculosis, and lung cancer by analyzing chest radiographs.

EfficientNet's compound scaling algorithm strikes a compromise between network depth, breadth, and resolution. This approach entails simultaneously growing its depth, breadth, and resolution to construct a sequence of models from EfficientNetB0 to EfficientNetB7, with B7 being the largest and most powerful [16]. The model has been used to detect and classify anomalies in mammogram images. In this application, the model helps identify potential signs of breast cancer by analyzing mammographic data [17].

2. PROPOSED METHOD

The conceptual background for this research as illustrated in Figure 1. The proposed method follows the Knowledge Discovery in Databases (KDD), which consists of domain understanding, data acquisition and understanding, data processing, modelling, evaluation and deployment [18], [19].

The selected images were mutually exclusive from recognized and benchmarked dataset. The NIH Chest X-ray 14 dataset contains over 100,000 frontal-view X-ray images of 32,717 unique patients. The images are labelled with 14 different thoracic disease conditions, making it a significant resource for training and evaluating machine learning models in medical imaging and disease detection. The dataset is widely used for research in radiology and machine learning [9].

The dataset "Chest X-ray Images (Pneumonia)" on Kaggle comprises 5,863 tagged chest X-ray images divided into three categories: normal, bacterial, and viral. It is separated into training, testing, and validation sets, with photos obtained from paediatric children aged one to five at the Guangzhou Women and Children's Medical Centre. The dataset is commonly used for training and evaluating machine-learning models in medical imaging and disease detection [20].

The input size of the three models used was 224×224 pixels, a standard dimension for many image classification tasks, including those involving medical imagery. This inputs size balances, maintaining sufficient image detail and ensuring manageable computational requirements. The chosen input size allows the model to capture relevant features in chest X-ray images, such as patterns indicative of thoracic diseases, while also keeping the processing time feasible for practical use.

Pre-trained ImageNet weights were used for all three models. Training the model with these weights provides a significant advantage by leveraging transfer learning. ImageNet, a large dataset with over a million images across a thousand categories, offers a rich feature representation that can be repurposed for different tasks. By starting with these pre-trained weights, the model benefits from a well-established foundation of learned features, enabling it to converge faster and achieve higher accuracy with fewer training examples specific to thoracic diseases. This approach is particularly beneficial in medical imaging, where annotated data can be scarce and expensive.

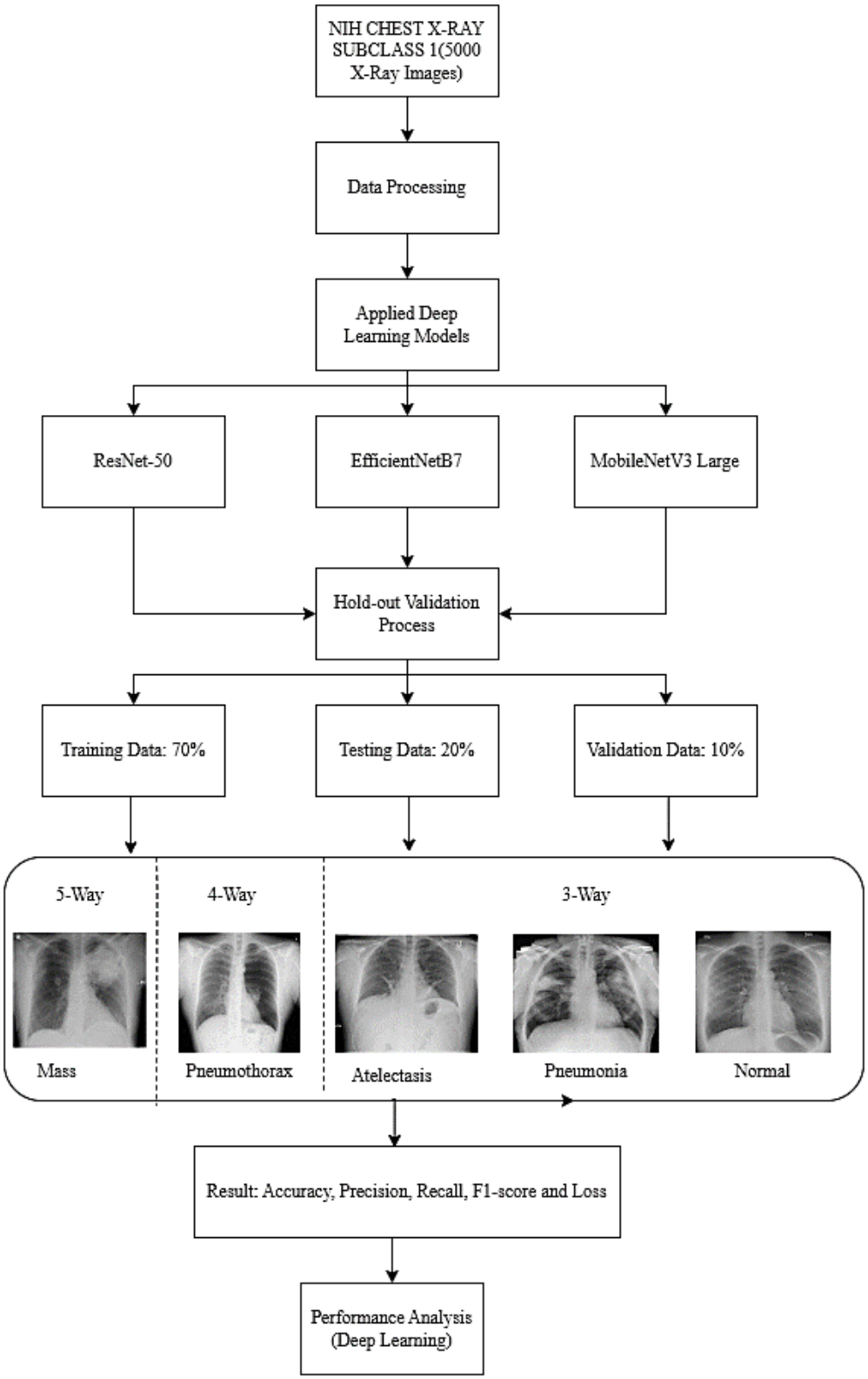

Figure 1. Conceptual framework of the developed model

Table 1 shows the description of the dataset with atelectasis mass, pneumonia, pneumothorax and normal with equal total number of classes, training, validation, and testing data of 1500, 1050, and 300 respectively.

Table 1. Description of dataset

Classes	Total number of CXIs/class	Training set	Validation set	Testing set
Atelectasis	1500	1050	150	300
Mass	1500	1050	150	300
Pneumonia	1500	1050	150	300
Pneumothorax	1500	1050	150	300
Normal	1500	1050	150	300

The layers introduced to the MobileNetV3Large architecture are carefully chosen to customize the model for the specific objective of thoracic illness categorization. The Flatten() layer converts the multi-dimensional output from the base model into a one-dimensional vector. This transition from convolutional layers to fully connected layers is crucial for preparing the data for classification by the dense layers that follow. The first Dense(256, activation=swish) layer introduces 256 fully connected neurons with the Swish activation function. The Swish activation function as defined by (1):

$$f(x) = x \cdot sigmoid(x) \quad (1)$$

is known for its smooth and non-monotonic nature, allowing the model to learn complex, non-linear data representations. This enhances the model's ability to capture intricate patterns in the chest X-ray images.

Dropout(0.5) is a regularization approach for avoiding overfitting. Dropout improves model generalizability to new data by randomly setting 50% of neurons to zero during each training cycle. This is especially essential in medical imaging jobs since models can quickly recall training data. Dense Layer (128 units, Swish activation): The second Dense(128, activation=swish) layer adds another set of fully connected neurons, further increasing the model's capacity to learn complex features from the data. The Swish activation function is again employed here to take advantage of its superior performance in deep learning tasks. Dropout layer (50%): another Dropout(0.5) layer is included to maintain the regularization effect, ensuring consistent overfitting prevention as the model continues to learn.

Output layer: the final Dense(K, activation="softmax", kernel_regularizer=l2(0.001)) layer produces probability distributions over the dataset's K classes of thoracic diseases. The SoftMax activation function ensures that the sum of the output probabilities equals one, allowing for clear and interpretable class predictions. The L2 regularization helps prevent overfitting by penalizing large weights, ensuring the model remains robust and generalizable.

This combination of layers at the end of the models' architecture ensures that the model can extract relevant features from the chest X-ray images and is adept at making accurate and reliable classifications. Using the Swish activation function, dropout for regularization, and L2 regularization in the output layer contributes to the model's enhanced performance in the specific task of thoracic disease classification, as shown in Figure 2, the transfer-learning pipeline.

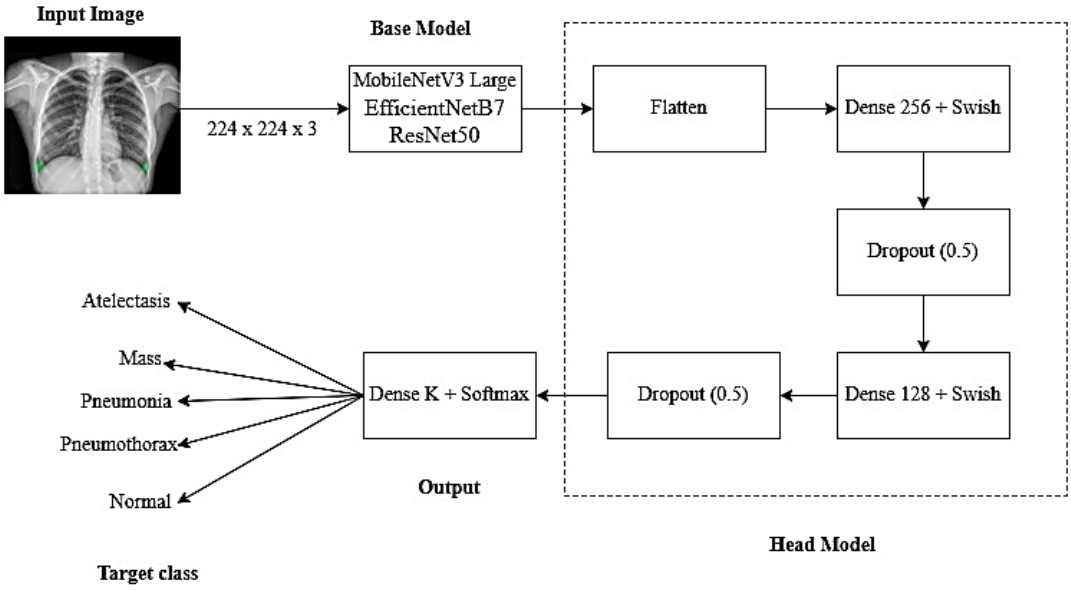

Figure 2. Transfer learning pipeline

The models will be assessed using four criteria: accuracy, recall, precision, specificity, and the F1-score. They are as specified in (2) to (5) [21]-[25]:

$$Accuracy = \frac{TP+TN}{TP+TN+FP+FN} \quad (2)$$

$$Precision = \frac{TP+TN}{TP+FP} \quad (3)$$

$$Recall = \frac{TP}{TP+FP} \quad (4)$$

$$F1\ Score = \frac{2*Precision*Recall}{Precision+Recall} \quad (5)$$

where: TP is true positive, TN is true negative, FN is false negative, and FP is false positive.

2.1. Environment and parameters settings

The Table 2 summarize the key training parameters and configurations used for different deep learning architectures: MobileNetV3Large, ResNet-50, and EfficientNetB7 across 5, 4, and 3-way classification. Each model is trained on a dataset of thoracic disease images using identical settings to ensure a fair comparison of their performance.

Table 2. Parameters settings

Parameters	MobileNetV3Large	ResNet-50	EfficientNetB7
Image size	224×224	224×224	224×224
Batch size	64	64	64
Epoch	20	20	20
Patience	3	3	3
Learning rate	0.0010	Scheduler	Scheduler
Optimizer	Adam	Adam	Adam
Loss	Categorical cross-entropy	Categorical cross-entropy	Categorical cross-entropy
Training split	0.7	0.7	0.7
Validation split	0.1	0.1	0.1
Testing split	0.2	0.2	0.2
Callbacks	EarlyStopping	EarlyStopping	EarlyStopping

The training environment was done in:

- HP Pavilion Laptop 15-cc0xx;
- Microsoft Windows 11 Pro 64-bit;
- Intel(R) Core(TM) i5-7200U CPU @ 2.50GHz with a max clock speed of 2712;
- 4-partitioned SSD of 256052966400 bytes Storage (Model: MTFDDAV256TBN-1AR15ABHA).

2.2. Model integration into web and mobile applications

The developed deep learning model can be used for practical purposes after a successful model evaluation. Potential integration scenarios include incorporating the model into:

- Software for medical imaging analysis would enable practitioners to use the model's categorization powers in their current procedures.
- Web application: a web application has been developed to offer a user-friendly platform for eye disease classification activities.

2.2.1. Testing application

A Python script was made to implement a graphical user interface (GUI) using Tkinter to facilitate the loading and testing of Keras models on chest X-ray images to classify thoracic diseases. The application consists of several key components:

- Libraries and dependencies: the code imports necessary libraries such as Tkinter for the GUI, TensorFlow for loading and processing the model, and PIL for image handling. ImageDataGenerator from Keras is used to apply data augmentation techniques and preprocess the input images.
- Image data generator: an ImageDataGenerator object is created with specified augmentation parameters like rotation, width shift, height shift, and zoom range. This helps to enhance the model's robustness by providing varied training examples.

- GUI elements: the main application window is initialised with buttons for loading the Keras model and image files. Labels are used to display the selected image and the prediction results. Functions load_model_file and load_image_file allow the user to select a model and an image file, respectively. The selected image is displayed in a thumbnail format within the application.
- Image preprocessing: the preprocess_image function uses a temporary DataFrame and the ImageDataGenerator to preprocess the selected image, ensuring it matches the input requirements of the model.
- Model prediction: the run test function is the core of the testing process. It preprocesses the loaded image and uses the loaded model to make a prediction. The predicted probabilities and class names are displayed to the user.
- User interaction: the application provides feedback to the user via message boxes, indicating the success or failure of model loading, image loading, and the test run.

This testing application provides a user-friendly interface for evaluating the performance of Keras models on chest X-ray images, aiding in the classification of thoracic diseases.

2.2.2. Web application for classifying thoracic diseases

With the help of a pre-trained deep learning model, users of this programmed can submit chest X-rays and receive diagnoses of eye diseases. It blends two essential components:

- JavaScript Frontend: Constructed using HTML, CSS, and JavaScript, the front end offers an intuitive user experience. Users can:

a. Upload an image using a specific element.
b. Press a button to start the classification process.
c. Examine the classification outcomes as a table or list.

In the background, JavaScript takes a picture of the submitted file and compresses it (base64) for faster transmission. Makes use of an AJAX request to provide the data to the backend.

- Flask backend: the backend runs server-side processes and is Flask-powered. It gets the frontend's base64-encoded picture data; It decodes the data back into the original format; the trained deep learning model is loaded. Generates predictions on the image using the model. Prepares a response with the highest projected classes together with confidence ratings. Returns the response in JSON format to the front end.

3. RESULTS AND DISCUSSION

3.1. Results

3.1.1. Results in terms of accuracies and loses

Confusion matrix analysis was utilised to assess the performance of the classification models and provide insights into their behaviour. The confusion matrix has two sorts of elements: diagonal and off diagonal. The diagonal elements show occasions when the predicted labels matched the actual labels, suggesting proper classifications. Off-diagonal elements describe occasions when the classifier mislabelled or misclassified the data.

The larger the diagonal values in the confusion matrix, the more accurate the predictions the model made conversely, the smaller the off-diagonal values, the fewer instances where the model misclassified the data. The confusion matrix provides a comprehensive view of the model's classification performance across the different classes.

The training and validation, accuracies and losses experience during the dataset processing with the three different architectures are represented in Figures 3-5. While Figures 6-8 displayed the confusion matrixes of the models with the class. Across all epochs, the MobileNetV3Small model had the lowest training loss and the highest training accuracy, indicating that the lung disease data was trained effectively on the MobileNetV3 architecture.

The algorithm was trained to identify and categorize verified lung disease patients using chest X-ray pictures. To remove any bias effects, the dataset was created by randomly picking an evenly distributed set of chest X-rays from multiple sources. Separate datasets were utilised for training, validation, and testing. Notably, the test dataset was unknown to the model beforehand, ensuring that the model performs excellently on new, unseen data.

The implementation for categorizing lung disease cases into five subclasses was trained and validated. The model was trained for 20 epochs for all five subclasses with a batch size of 64. The study findings for the five subclasses of lung-related disorders, utilizing a balanced dataset and a deep feature extraction methodology, are shown here.

The confusion matrix for the 5-subclass lung-related disease classification using the MobileNetV3Small model is presented in Figures 6-8. The results show that pneumonia and pneumothorax

achieved better classification performance than the other disease classes. This model can accurately identify the occurrence of specific thoracic diseases, enabling patients to quickly take appropriate precautions. In addition, the classification performance measures accuracy, recall, and F1-score were determined for each illness class for each model and class. The general overview of each model's results is as illustrated in Table 3.

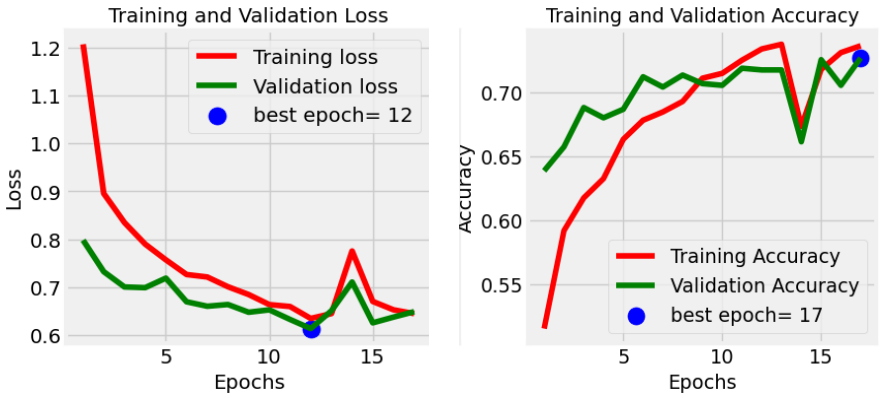

Figure 3. EfficientNetB7's performance for training and validation accuracy and loss on 5 subclasses

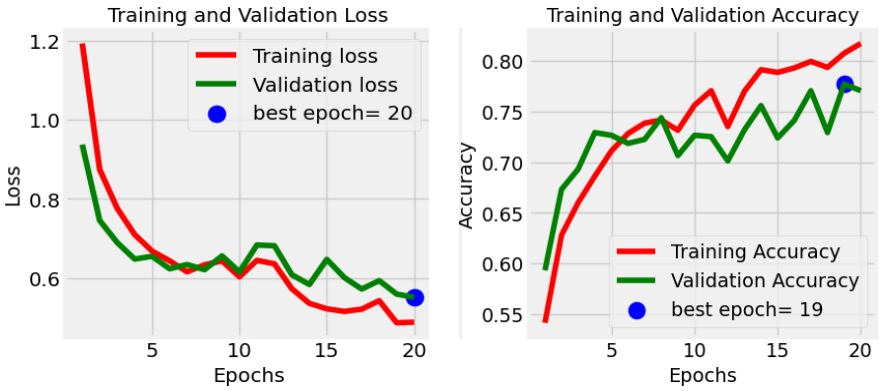

Figure 4. ResNet-50's performance for training and validation accuracy and loss on 5 subclasses

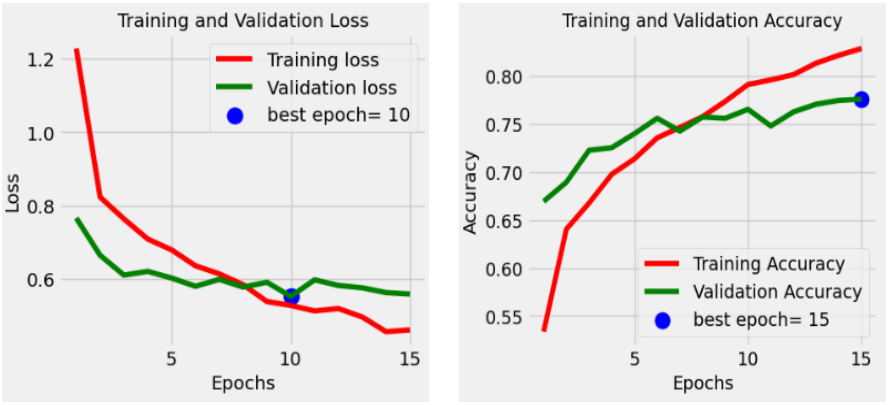

Figure 5. MobileNetV3's performance for training and validation accuracy and loss on 5 subclasses

Table 3. Comparative analysis of various models

Subclass	Metrics	Disease	MobileNetV3Large (%)	ResNet50 (%)	EfficientNetB7 (%)
5-way classification	Accuracy		**75.72**	75.2	73.03
	Precision	Atelectasis	55.71	57.91	**61.39**
		Mass	59.46	**60.64**	50.29
		Pneumonia	**97.01**	92.49	93.04
		Pneumothorax	**80.32**	75.97	69.11
		Normal	94.5	94.40	**96.02**
	Recall	Atelectasis	**80.74**	67.83	63.39
		Mass	59.66	**72.15**	57.81
		Pneumonia	94.49	94.02	**96.56**
		Pneumothorax	46.51	47.22	**56.29**
		Normal	**96.83**	92.88	93.66
	F1-score	Atelectasis	**65.93**	62.47	62.37
		Mass	59.56	**65.89**	53.79
		Pneumonia	**95.73**	93.24%	94.77
		Pneumothorax	58.91	58.24	**62.04**
		Normal	**95.65**	93.64	94.82
4-way classification	Accuracy		87.25	87.08	**88.08**
	Precision	Atelectasis	76.76	**78.95**	76.53
		Pneumonia	**97.32**	92.15	96.79
		Pneumothorax	79.25	81.17	**83.98**
		Normal	95.93	**97.74**	97.05
	Recall	Atelectasis	76.48	80.00	**87.26**
		Pneumonia	96.67	**97.9**	96.45
		Pneumothorax	79.01	**80.43**	71.9
		Normal	**97.25**	91.23	97.05
	F1-score	Atelectasis	76.62	79.47	**81.54**
		Pneumonia	**96.99**	94.93	96.61
		Pneumothorax	79.13	**80.79**	77.47
		Normal	96.58	94.38	**97.05**
3-way classification	Accuracy		97.44	**97.88**	96.55
	Precision	Atelectasis	**100**	99.66	99.3
		Pneumonia	96.56	**97.46**	95.03
		Normal	95.69	**96.57**	95.49
	Recall	Atelectasis	**100**	99.65	99.3
		Pneumonia	95.58	**96.84**	95.67
		Normal	96.65	**97.24**	94.89
	F1-score	Atelectasis	**100**	99.65	99.3
		Pneumonia	96.07	**97.15**	95.35
		Normal	96.17	**96.9**	95.19

3.1.2. Results in terms of confusion matrices

In addition to the MobileNetV3Small results, Figures 6(a)-(c) present the confusion matrices for the ResNet-50 and InceptionV3 models. These results indicate that the ResNet-50 and EfficientNetB7 models also exhibit good classification performance for the various thoracic-related disease classes.

The MobileNetV3, ResNet50, and EfficientNetB7 architectures were trained on a total dataset of 7,500 chest X-ray images, covering four thoracic-related diseases and normal: atelectasis, mass, pneumonia, normal, and pneumothorax. Each subclass contained 1,500 images, with the dataset divided in a 70:30 ratio for training and testing. The training dataset was further split into training and validation sets.

Figure 7(a) depicts the confusion matrix for the MobileNetV3 model's 4-subclass categorization of thoracic-related disorders. Similarly, Figure 7(b) depicts the confusion matrix for the ResNet50 model's 4-subclass categorization of lung illnesses. Finally, Figure 7(c) shows the confusion matrix for EfficientNetB7's 4-subclass categorization of thoracic-related disorders. These confusion matrices give a thorough breakdown of the classification performance for each of the thoracic-related illness subtypes across all three-model architectures.

Figures 8 present the confusion matrices corresponding to the 4-class classification of thoracic-related disorders using three distinct deep learning models. Specifically, Figure 8(a) illustrates the classification performance of the MobileNetV3 model, while Figure 8(b) shows the confusion matrix for the ResNet50 architecture applied to the same 4-subclass problem. In parallel, Figure 8(c) displays the performance of EfficientNetB7 in categorizing thoracic-related diseases. These visual representations collectively offer a comprehensive comparison of how each model distinguishes between the four thoracic illness subtypes, highlighting their relative strengths and misclassification patterns.

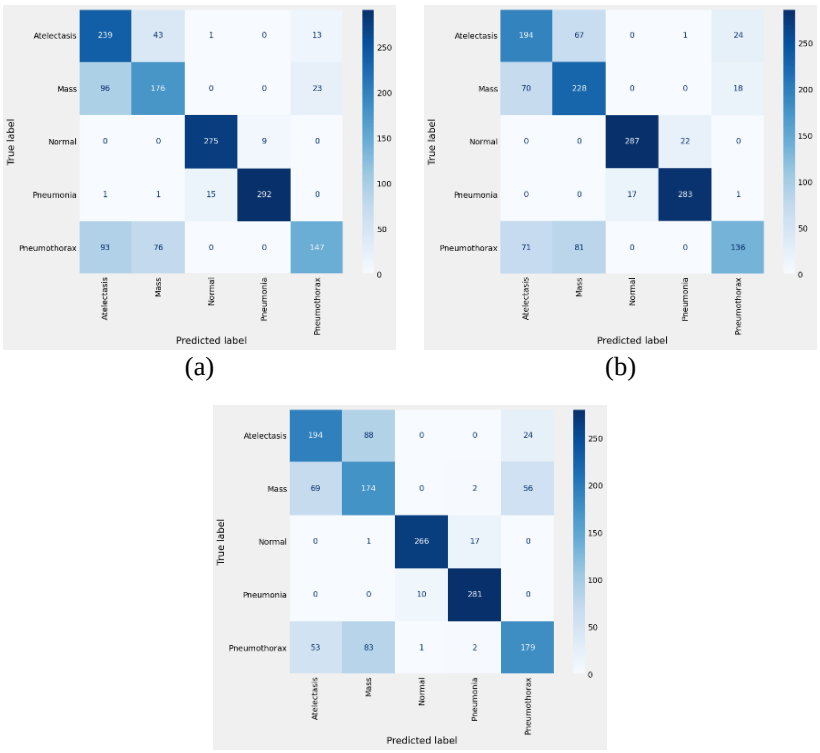

(a) (b)

(c)

Figure 6. Confusion matrix visualizing performance on classifying 5-subclasses of; (a) MobileNetV3, (b) ResNet-50, and (c) EfficientNetB7

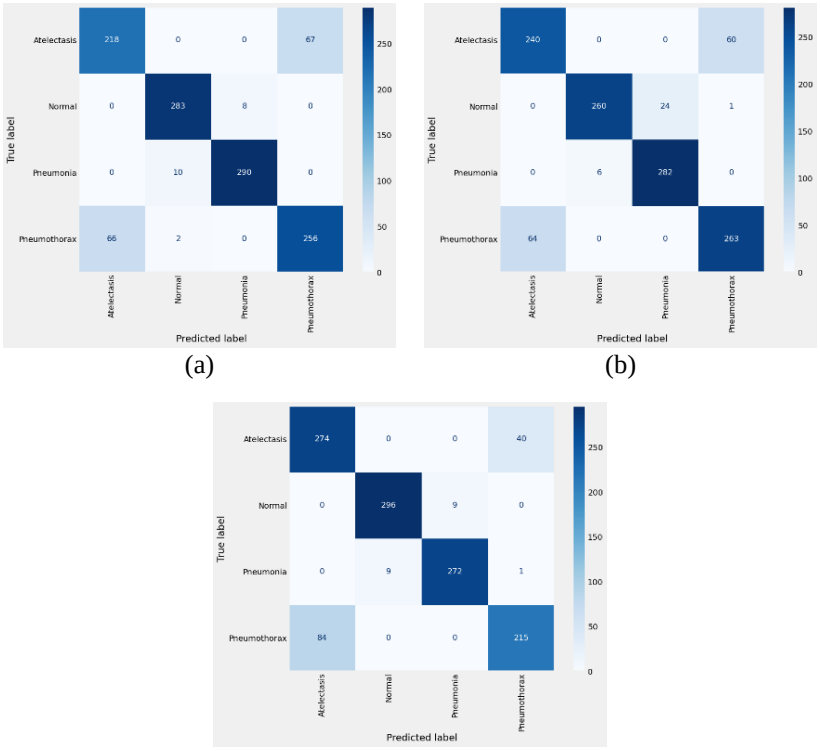

(a) (b)

(c)

Figure 7. Confusion matrix visualizing performance on classifying 4-subclasses of; (a) MobileNetV3, (b) ResNet-50, and (c) EfficientNetB7

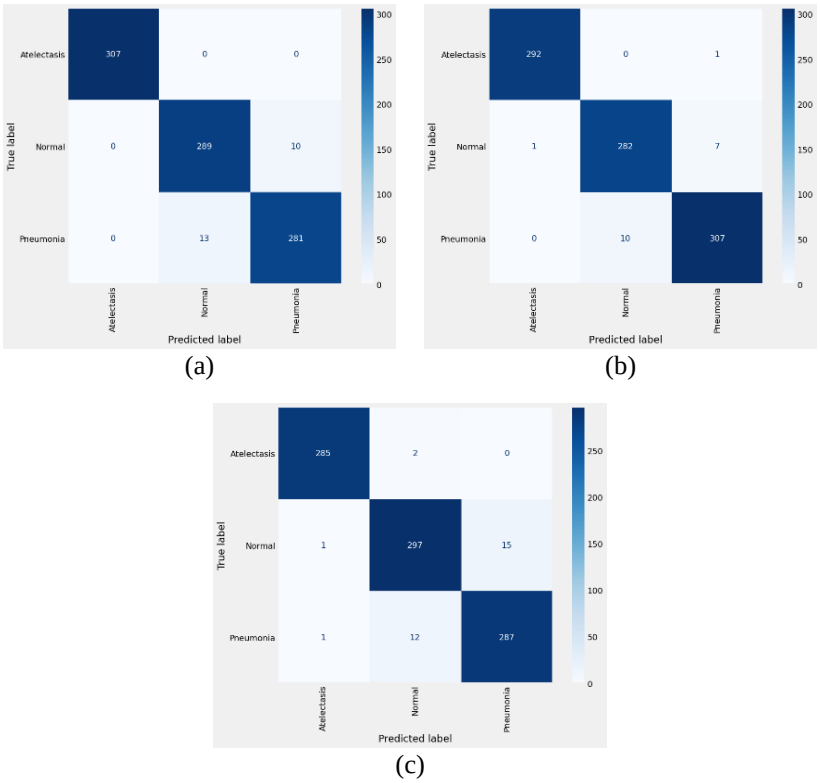

(a) (b)

(c)

Figure 8. Confusion matrix visualizing performance on classifying 3-subclasses of; (a) MobileNetV3, (b) ResNet-50, and (c) EfficientNetB7

3.2. Discussion

Several key insights emerge from the comparison in evaluating the three deep learning models across the 5-way, 4-way, and 3-way classifications. MobileNetV3Large, ResNet50, and EfficientNetB7 demonstrate varying performance levels across different metrics and diseases, providing a comprehensive view of their strengths and weaknesses. These key insights and the comparative analysis of the various models are show in Table 3.

For the 5-way classification, which includes diseases such as atelectasis, mass, pneumonia, and pneumothorax, MobileNetV3Large achieves an overall accuracy of 75.72%, slightly outperforming ResNet50's 75.20% but trailing behind EfficientNetB7's 73.03%. Regarding precision, MobileNetV3Large and ResNet50 display close performance in Atelectasis with values of 55.71% and 57.91%, respectively, while EfficientNetB7 excels at 61.39%. However, ResNet50 performs better in precision for diseases like mass and pneumonia than the other two models, with scores of 60.64% and 92.49%, respectively, highlighting its robustness in these specific classifications.

The models show improved overall accuracy in the 4-way classification, which omits one disease from the previous set. MobileNetV3Large achieves an accuracy of 87.25%, closely matched by ResNet50 at 87.08%, but both are surpassed by EfficientNetB7 at 88.08%. The precision metric for pneumonia is particularly noteworthy, where MobileNetV3Large scores 97.32%, closely followed by EfficientNetB7 at 96.79% and ResNet50 at 92.15%, indicating strong performance across the board. For Normal cases, ResNet50 stands out with a precision of 97.74%, while MobileNetV3Large and EfficientNetB7 are close behind at 95.93% and 97.05%, respectively.

In the 3-way classification, which further simplifies the categorisation, all models show significantly higher accuracy and precision. MobileNetV3Large achieves an accuracy of 97.44%, ResNet50 slightly higher at 97.88%, and EfficientNetB7 at 96.55%. Precision for Atelectasis is perfect for MobileNetV3Large and ResNet50, achieving 100%, while EfficientNetB7 is close at 99.30%. Pneumonia precision remains high across all models, with ResNet50 leading at 97.46%, MobileNetV3Large at 96.56%, and EfficientNetB7 at 95.03%. For the Normal classification, ResNet50 again shows superior performance with 96.57% precision, compared to MobileNetV3Large's 95.69% and EfficientNetB7's 95.49%.

Generally, MobileNetV3Large and ResNet50 perform closely, with ResNet50 often-showing slightly better precision in more complex classifications. EfficientNetB7, while generally trailing in precision, shows competitive accuracy and robustness across different classification scenarios.

4. CONCLUSION

Key findings highlighted the superior performance of MobileNetV3Large in terms of computational efficiency and accuracy, particularly when enhanced with transfer learning and attention mechanisms. ResNet50 showed robust performance across different disease classifications, often surpassing the other models in precision for complex classifications. EfficientNetB7 demonstrated competitive accuracy, highlighting its robustness in various classification scenarios.

The integration of attention mechanisms within these architectures significantly improved diagnostic precision by focusing on critical regions of the chest X-ray images. This approach reduced the dependency on radiologists and democratized access to high-quality diagnostic tools, especially in resource-constrained settings. The study underscores the transformative potential of AI in medical imaging, paving the way for future advancements in AI-powered healthcare. Recommendations for future research include further refinement of these models, exploring additional data augmentation techniques, and implementing more advanced explainable AI techniques to foster trust and clinical adoption.

ACKNOWLEDGMENTS

The authors appreciate substantial support from the Covenant University Centre for Research, Innovation, and Discovery (CUCRID), Ota, Ogun State, Nigeria.

FUNDING INFORMATION

No funding involved.

AUTHOR CONTRIBUTIONS STATEMENT

This journal uses the Contributor Roles Taxonomy (CRediT) to recognize individual author contributions, reduce authorship disputes, and facilitate collaboration.

Name of Author	C	M	So	Va	Fo	I	R	D	O	E	Vi	Su	P	Fu
Kennedy Okokpujie	✓	✓	✓	✓	✓	✓	✓	✓	✓	✓	✓	✓	✓	✓
Tamunowunari-Tasker Anointing	✓	✓	✓	✓	✓	✓	✓	✓	✓	✓	✓		✓	
Adaora Princess Ijeh		✓					✓		✓	✓	✓		✓	✓
Imhade Princess Okokpujie		✓					✓			✓	✓		✓	✓
Mary Oluwafeyisayo Ogundele				✓	✓		✓			✓			✓	
Oluwadamilola Oguntuyo						✓	✓		✓				✓	✓

C : **C**onceptualization
M : **M**ethodology
So : **So**ftware
Va : **Va**lidation
Fo : **Fo**rmal analysis
I : **I**nvestigation
R : **R**esources
D : **D**ata Curation
O : Writing - **O**riginal Draft
E : Writing - Review & **E**diting
Vi : **Vi**sualization
Su : **Su**pervision
P : **P**roject administration
Fu : **Fu**nding acquisition

CONFLICT OF INTEREST STATEMENT

No conflict of interest.

DATA AVAILABILITY

The data supporting this study's findings are openly available in the Kaggle repository at: https://www.kaggle.com/datasets/paultimothymooney/chest-xray-pneumonia [21].

REFERENCES

[1] World Health Organization, "Pneumonia," WHO. [Online]. Available: https://www.who.int/news-room/fact-sheets/detail/pneumonia. (Date accessed: Jun. 12, 2024).

[2] R. Khan and T. Mehmood, "Classification of Thoracic Diseases Based on Chest X-ray Images Using Kernel Support Vector Machine," *Mathematical Problems in Engineering*, pp. 1–9, 2022, doi: 10.1155/2022/9457730.
[3] Y. Akhter, R. Singh, and M. Vatsa, "AI-based radiodiagnosis using chest X-rays: A review," *Frontiers in Big Data*, vol. 6, pp. 1–27, 2023, doi: 10.3389/fdata.2023.1120989.
[4] A. A. Nasser and M. A. Akhloufi, "Deep Learning Methods for Chest Disease Detection Using Radiography Images," *SN Computer Science*, vol. 4, no. 4, 2023, doi: 10.1007/s42979-023-01818-w.
[5] T. Rahman *et al.*, "Transfer learning with deep Convolutional Neural Network (CNN) for pneumonia detection using chest X-ray," *Applied Sciences*, vol. 10, no. 9, pp. 1–17, May 2020, doi: 10.3390/app10093233.
[6] A. H. Al-Timemy, R. N. Khushaba, Z. M. Mosa, and J. Escudero, "An Efficient Mixture of Deep and Machine Learning Models for COVID-19 and Tuberculosis Detection Using X-Ray Images in Resource Limited Settings," *Studies in Systems, Decision and Control*, vol. 358, pp. 77–100, 2021, doi: 10.1007/978-3-030-69744-0_6.
[7] A. Sharma and P. K. Mishra, "Image enhancement techniques on deep learning approaches for automated diagnosis of COVID-19 features using CXR images," *Multimedia Tools and Applications*, vol. 81, no. 29, pp. 42649–42690, Dec. 2022, doi: 10.1007/s11042-022-13486-8.
[8] Z. Xue *et al.*, "Chest X-ray Image View Classification," *2015 IEEE 28th International Symposium on Computer-Based Medical Systems*, Sao Carlos, Brazil, 2015, pp. 66-71, doi: 10.1109/CBMS.2015.49.
[9] X. Wang, Y. Peng, L. Lu, Z. Lu, M. Bagheri, and R. M. Summers, "ChestX-ray8: Hospital-scale chest X-ray database and benchmarks on weakly-supervised classification and localization of common thorax diseases," in *2017 IEEE Conference on Computer Vision and Pattern Recognition (CVPR)*, Honolulu, HI, USA, Jul. 2017, pp. 3462–3471. doi: 10.1109/CVPR.2017.369.
[10] Q. Guan and Y. Huang, "Multi-label chest X-ray image classification via category-wise residual attention learning," *Pattern Recognition Letters*, vol. 130, pp. 259–266, Feb. 2020, doi: 10.1016/j.patrec.2018.10.027.
[11] J. O. Olayiwola, J. A. Badejo, K. Okokpujie, and M. E. Awomoyi, "Lung-Related Diseases Classification Using Deep Convolutional Neural Network," *Mathematical Modelling of Engineering Problems*, vol. 10, no. 4, pp. 1097–1104, Aug. 2023, doi: 10.18280/mmep.100401.
[12] A. Howard *et al.*, "Searching for mobilenetv3," in *Proceedings of the IEEE/CVF International Conference on Computer Vision (ICCV)*, 2019, pp. 1314–1324.
[13] M. A. Eshraghi, A. Ayatollahi, and S. B. Shokouhi, "COV-MobNets: a mobile networks ensemble model for diagnosis of COVID-19 based on chest X-ray images," *BMC Medical Imaging*, vol. 23, no. 1, pp. 1–14, 2023, doi: 10.1186/s12880-023-01039-w.
[14] K. H. Shibly, S. K. Dey, M. T. U. Islam, and M. M. Rahman, "COVID faster R–CNN: A novel framework to Diagnose Novel Coronavirus Disease (COVID-19) in X-Ray images," *Informatics in Medicine Unlocked*, vol. 20, pp. 1–9, 2020, doi: 10.1016/j.imu.2020.100405.
[15] K. He, X. Zhang, S. Ren, and J. Sun, "Deep residual learning for image recognition," in *Proceedings of the IEEE Conference on Computer Vision and Pattern Recognition (CVPR)*, 2016, pp. 770–778, doi: 10.1109/CVPR.2016.90.
[16] J. Wang, Y. Lu, L. Ma, and X. Jin, "Chest X-ray pneumonia recognition using a deep residual learning network," *IEEE Access*, vol. 9, pp. 24680–24687, 2019.
[17] M. Tan and Q. V. Le, "EfficientNet: Rethinking model scaling for convolutional neural networks," *International Conference on Machine Learning*, 2019, pp. 10691–10700.
[18] A. Giełczyk, A. Marciniak, M. Tarczewska, and Z. Lutowski, "Pre-processing methods in chest X-ray image classification," *PLoS One*, vol. 17, no. 4, 2022, doi: 10.1371/journal.pone.0265949.
[19] K. Okokpujie, I. O. Nwokolo, A. V. Adenugba, and M. E. Awomoyi, "Development of a Machine Learning Based Fault Detection Model for Received Signal Level in Telecommunication Enterprise Infrastructure," *International Journal of Safety and Security Engineering*, vol. 14, no. 3, pp. 679–690, Jun. 2024, doi: 10.18280/ijsse.140302.
[20] W. M. Salama and M. H. Aly, "Deep learning in mammography images segmentation and classification: Automated CNN approach," *Alexandria Engineering Journal*, vol. 60, no. 5, pp. 4701–4709, 2021, doi: 10.1016/j.aej.2021.03.048.
[21] P. Mooney, "Chest X-Ray Images (Pneumonia)," Kaggle. [Online]. Available: https://www.kaggle.com/datasets/paultimothymooney/chest-xray-pneumonia. (Date accessed: Jun. 21, 2024).
[22] K. Okokpujie, I. P. Okokpujie, O. I. Ayomikun, A. M. Orimogunje, and A. T. Ogundipe, "Development of a Web and Mobile Applications-Based Cassava Disease Classification Interface Using Convolutional Neural Network," *Mathematical Modelling of Engineering Problems*, vol. 10, no. 1, pp. 119–128, Feb. 2023, doi: 10.18280/MMEP.100113.
[23] T. Singh, S. Mishra, R. Kalra, Satakshi, M. Kumar, and T. Kim, "COVID-19 severity detection using chest X-ray segmentation and deep learning," *Scientific Reports*, vol. 14, no. 1, pp. 1-15, 2024, doi: 10.1038/s41598-024-70801-z.
[24] T. Ozturk, M. Talo, E. A. Yildirim, U. B. Baloglu, O. Yildirim, and U. R. Acharya, "Automated detection of COVID-19 cases using deep neural networks with X-ray images," *Computers in Biology and Medicine*, vol. 121, pp. 1–11, Jun. 2020, doi: 10.1016/j.compbiomed.2020.103792.
[25] S. Mohan, C. Thirumalai, and G. Srivastava, "Effective heart disease prediction using hybrid machine learning techniques," *IEEE Access*, vol. 7, pp. 81542–81554, 2019, doi: 10.1109/ACCESS.2019.2923707.

BIOGRAPHIES OF AUTHORS

Dr. Kennedy Okokpujie holds a Bachelor of Engineering (B.Eng.) in Electrical and Electronics Engineering, Master of Science (M.Sc.) in Electrical and Electronics Engineering, Master of Engineering (M.Eng.) in Electronics and Telecommunication Engineering and Master of Business Administration (MBA), Ph.D. in Information and Communication Engineering, besides several professional certificates and skills. He is currently an associate professor in the Department of Electrical and Information Engineering at Covenant University, Ota, Ogun State, Nigeria. He is a member of the Nigerian Society of Engineers and a senior member of the Institute of Electrical and Electronics Engineers (SMIEEE). His research areas of interest include biometrics, artificial intelligence, and network security and management. He can be contacted at email: kennedy.okokpujie@covenantuniversity.edu.ng and kenjie451@gmail.com.

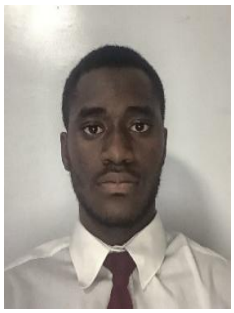

Tamunowunari-Tasker Anointing holds a Bachelor of Engineering (B.Eng.) degree in Information and Communication Engineering from Covenant University, Ota, Nigeria. He is an artificial intelligence enthusiast and his research areas of interest include machine learning, digital image processing, computer vision, and the internet of things. He can be contacted at email: anointing.tasker@stu.cu.edu.ng.

Adaora Princess Ijeh is a postgraduate student currently pursuing a Master's degree in Computer Science. She holds a Bachelor's degree in Computer Science from the Federal University of Petroleum Resources, Effurun, Delta State, Nigeria. For her undergraduate research, she developed a web-based electronic management application aimed at improving administrative efficiency. Her current research interests include cybersecurity and artificial intelligence, with a focus on developing smart, data-driven systems. She is dedicated to advancing intelligent technologies through secure and innovative software solutions. She aspires to contribute to cutting-edge research in intelligent systems and secure software design, with the long-term goal of enhancing digital infrastructure in both developing and developed regions. She can be contacted at email: adaora.ijehpgs@stu.cu.edu.ng.

Dr. Imhade Princess Okokpujie an Associate Professor at Afe Babalola University, holds a Ph.D. in Mechanical Engineering from Covenant University, focusing on nano-lubricant in advanced manufacturing. She has authored over 186 scholarly papers and a book on modern optimization techniques. She has secured three research grants and received multiple awards, including Covenant University's Chancellor's Exceptional Researcher of the Year (2018, 2019) and Afe Babalola University's outstanding research award. She specializes in advanced manufacturing, nano-lubricants, and energy systems, and has been awarded the Global Excellence Stature Fellowship Grant at the University of Johannesburg. A registered COREN engineer and NSE member, she has held leadership roles in her Institution, APWEN and NSE, mentoring numerous students and young researchers. She is passionate about girl-child education and women's development. She can be contacted at email: ip.okokpujie@abuad.edu.ng.

Mary Oluwafeyisayo Ogundele holds a B.Sc. in Electronics and Computer Engineering, a Master's degree in Information Technology and a Masters of Business Administration (MBA) amongst other professional certifications. She currently leads the Network and User Administration Team at Unified Payments Systems, a prominent fintech organization in Nigeria. She served at Nigeria's Apex Bank, where she was responsible for administering and managing critical network and security solutions. She is a member of the Nigeria Society of Engineers (NSE), Council for the Regulation of Engineering in Nigeria (COREN) and a fellow of The National Institute of Professional Engineers and Scientists (NIPES). She can be contacted at email: sayoo_22@yahoo.com.

Oluwadamilola Oguntuyo is a student of College of the Holy Cross, Worcester, Massachusetts majoring in Mathematics with a minor in Statistics. As a research student, she is deeply passionate about exploring and applying mathematical concepts to address real world challenges. Her work reflects a strong commitment to analytical thinking, problem solving, and advancing knowledge in the field. She can be contacted at email: damilolalawani3@gmail.com.